# Coupled vibroacoustic finite element model of the sound production of the xylophone

Mihály Ádám Ulveczki[1], Péter Rucz[1]

[1] *Budapest University of Technology and Economics, Budapest, Hungary, Email: ulveczki.mihaly.adam@simonyi.bme.hu*

## INTRODUCTION

Computer-aided design and simulation-based virtual prototyping play an increasingly important role in the design and optimization of new musical instrument models. These methods help to create precisely tuned, high-quality products and also facilitate the preparation of series production. In the case of the xylophone, two elements have a decisive role in the sound emission of the instrument: the sound bar and the resonator, which interact with each other and with the excitation produced by the mallet. For modeling realistic geometries (irregular tuning cuts, or resonators of various shapes), numerical tools, such as the finite element method (FEM), are necessarily applied.

In this contribution the vibroacoustic behavior of the sound bars and resonators of a xylophone are investigated, first independently, and then in a coupled model considering the two-way interactions of these elements. The implementation is validated by means of various tests and also by comparison with measured data. The established fully coupled model can be utilized for virtual prototyping, and for synthesizing xylophone sounds, in addition. Finally, the influence of changing certain parameters of the system on the perceived sound is illustrated, highlighting the importance of two-way coupling between sound bars and resonators.

## COMPUTATIONAL MODEL

### Model of the sound bar

The sound bar model utilizes the mechanical FEM. The three-dimensional structured mesh is created starting with a brick which is then transformed geometrically to attain the actual undercut of the middle part, as can be seen in Figure 1. A linear elastic model with viscoelastic losses is used with an orthotropic representation of the material properties of the wooden bars. The finite element discretization results in an algebraic system of equations relating the excitation force $\mathbf{f}$ and the displacement response $\mathbf{u}$ as

$$(\mathbf{K}_\mathrm{m} + \mathrm{j}\omega\mathbf{C}_\mathrm{m} - \omega^2\mathbf{M}_\mathrm{m})\mathbf{u} = \mathbf{F}_\mathrm{m}\mathbf{f}, \qquad (1)$$

where $\mathbf{K}_\mathrm{m}$, $\mathbf{C}_\mathrm{m}$, $\mathbf{M}_\mathrm{m}$, and $\mathbf{F}_\mathrm{m}$ are the mechanical stiffness, damping, mass and excitation matrices and $\omega$ is the circular frequency.

To solve (1), modal superposition is exploited. The mode shapes and eigenfrequencies were calculated first, by solving (1) without any excitation and damping. The first vertical, horizontal and torsional bending mode of the F4 sound bar are also shown in Figure 1. Then, the displacement of the bar can be computed as a linear combination of the mode shapes as a response to any excitation. This modal solution approach is more efficient than solving (1) directly. It should be mentioned that this method in itself can only be applied if the excitation force is independent of the displacement of the sound bar, which is not true for the case of the mallet–sound bar interaction.

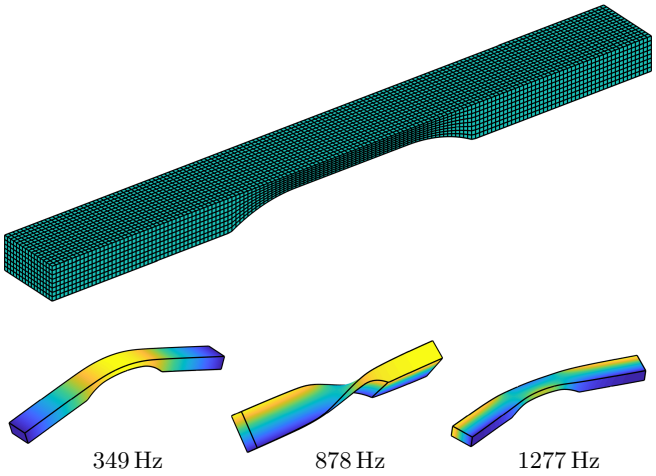


**Figure 1:** The model of the F4 sound bar (top) and the first mode shapes: vertical (bottom left), torsional (bottom middle) and horizontal (bottom right)

### Model of the resonator

Similar to the sound bar, the resonator is modelled by a 3D geometry, using the acoustical FEM based on the Helmholtz equation. The excitation of the acoustical system is the normal particle velocity $\mathbf{v}$ on the surfaces and the response is the sound pressure $\mathbf{p}$ in the whole domain:

$$(\mathbf{K}_\mathrm{a} + \mathrm{j}\omega\mathbf{C}_\mathrm{a} - \omega^2\mathbf{M}_\mathrm{a})\mathbf{p} = -\mathrm{j}\omega\mathbf{F}_\mathrm{a}\mathbf{v}. \qquad (2)$$

The challenge in the acoustical model is the treatment of the infinite domain, as the xylophone is assumed to radiate into free space. Figure 2 displays a truncated finite acoustical domain of a resonator. The acoustical mesh is subdivided into tetrahedra elements. To emulate free field radiation conditions infinite elements are utilized that are attached on the outer surface of the top cuboid visible in Figure 2. The infinite elements represent the decaying and oscillating propagation of sound waves towards infinity, such that incident waves are perfectly absorbed by them without any reflection. Our implementation follows the formulation given in [1]. It is also noted that the damping matrix $\mathbf{C}_\mathrm{a}$ arises due to the infinite elements.

### Vibroacoustic coupling

The mechanical and acoustical finite element models are coupled by taking two-way interactions into account. The sound pressure exerts force over the surfaces of the sound bar, and at the same time, the vibration of the bar results in a normal particle velocity excitation on

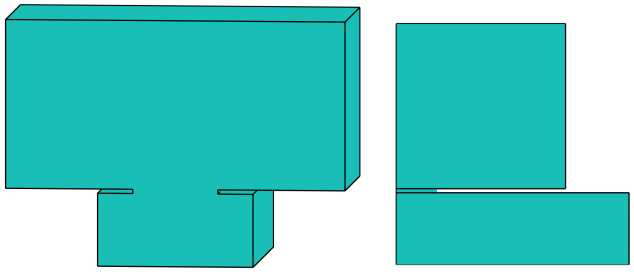

**Figure 2:** The model of a cavity resonator (bottom cuboid) with the simulated outer domain (top cuboid) in front view (left) and side view (right). The two domains are connected by a short neck. As the resonator has a symmetry plane, only a half model is meshed.

the interaction surface of the acoustical and mechanical models. The coupled equations read as

$$(\mathbf{K}_\mathrm{m} + \mathrm{j}\omega\mathbf{C}_\mathrm{m} - \omega^2\mathbf{M}_\mathrm{m})\mathbf{u} = \mathbf{F}_\mathrm{m}(\mathbf{f} + \mathbf{A}_\mathrm{m}\mathbf{p}) \quad (3)$$

$$(\mathbf{K}_\mathrm{a} + \mathrm{j}\omega\mathbf{C}_\mathrm{a} - \omega^2\mathbf{M}_\mathrm{a})\mathbf{p} = -\mathrm{j}\omega\mathbf{F}_\mathrm{a}(\mathbf{A}_\mathrm{a}\mathrm{j}\omega\mathbf{u}) \quad (4)$$

The matrices $\mathbf{A}$ project the displacement and the sound pressure between the finite elements of the two models by means of conservative interpolation. From (3)–(4) a block matrix equation can be written by rearranging the unknown $\mathbf{u}$ and $\mathbf{p}$ to the left hand side:

$$\mathbf{K}_\mathrm{c}\begin{bmatrix}\mathbf{u}\\ \mathbf{p}\end{bmatrix} + \mathrm{j}\omega\mathbf{C}_\mathrm{c}\begin{bmatrix}\mathbf{u}\\ \mathbf{p}\end{bmatrix} - \omega^2\mathbf{M}_\mathrm{c}\begin{bmatrix}\mathbf{u}\\ \mathbf{p}\end{bmatrix} = \begin{bmatrix}\mathbf{F}_\mathrm{m}\mathbf{f}\\ \mathbf{0}\end{bmatrix}. \quad (5)$$

The subscript $c$ refers to the coupled model and the block matrices can be expressed from the acoustical and mechanical system matrices. The solution of the coupled problem is attained by solving (5). The number of unknowns can be reduced by expressing both systems in a truncated modal basis. In the sequel the computation of the excitation force by the mallet, appearing in the vector $\mathbf{f}$, is discussed.

## Collision model

The interaction of the mallet and the sound bar can be modeled as an elastic collision of two spheres [2]. The Hertz law expresses the connection between the force $F$ acting on the mallet head and its compression $\delta_\mathrm{M}$

$$\delta_M = \left[F^2 D^2 \left(\frac{1}{r_\mathrm{B}} + \frac{1}{r_\mathrm{M}}\right)\right]^{\frac{1}{3}}, \quad (6)$$

where $r_\mathrm{B}$ and $r_\mathrm{M}$ are the radius of the two "spheres": that of the bar and of the mallet, respectively. The constant $D$ is derived from the material properties of the colliding objects. As the surface of the bar is nearly planar and its size is much greater than that of the mallet head, the limit $r_\mathrm{B} \to \infty$ is taken. In this case a non-linear relation of force and compression is attained:

$$F = \frac{\sqrt{r_\mathrm{M}}}{D}\delta_M^{\frac{3}{2}}. \quad (7)$$

Using (7), the equation of motion for the mallet head is written connecting the compression and the acceleration of the mallet head. Then, the motion of the mallet can be estimated by a suitable time stepping scheme.

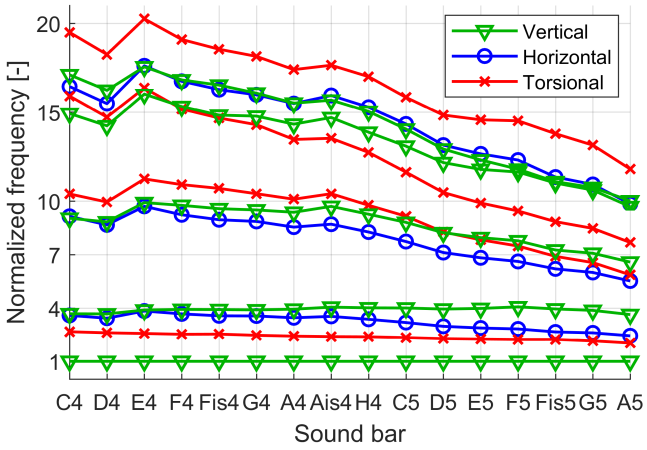


**Figure 3:** Mode frequencies of the 16 rosewood xylophone sound bars

## Interaction of mallet and sound bar

When in contact with the sound bar, the compression of the head results as the difference of the displacement of the mallet head and that of the bar in the position of the contact. Thus, the interaction needs to be calculated by solving the FEM equation (5) and the equation of motion for the mallet head simultaneously. However, the computation has to be done in time domain, due to the non-linear relation (7). Equation (5) reads in the time domain as

$$\mathbf{K}_\mathrm{c}\begin{bmatrix}\mathbf{u}\\ \mathbf{p}\end{bmatrix} + \mathbf{C}_\mathrm{c}\frac{\partial}{\partial t}\begin{bmatrix}\mathbf{u}\\ \mathbf{p}\end{bmatrix} + \mathbf{M}_\mathrm{c}\frac{\partial^2}{\partial t^2}\begin{bmatrix}\mathbf{u}\\ \mathbf{p}\end{bmatrix} = \begin{bmatrix}\mathbf{F}_\mathrm{m}\mathbf{f}\\ \mathbf{0}\end{bmatrix}. \quad (8)$$

Equation (8) is solved by the Newmark time stepping scheme [3] in a predictor–corrector manner. First, the interaction force is predicted based on the current displacement of the mallet and the sound bar. Then, the coupled system is solved with the predicted force, and finally, the dynamics of the mallet are corrected using the updated displacement of the sound bar. Using this method the vibration of the sound bar and the oscillations of the acoustical field are calculated both during interaction and free vibration for all time steps.

# RESULTS

## Modal behavior of the sound bars

The most important information about the vibration of the sound bars are the eigenfrequencies and the mode shapes. Figure 3 shows the relative frequencies of the first few eigenmodes, where the vertical axis is normalized by the frequency of the first vertical mode of each sound bar.

First, the computations were performed using the orthotropic elastic parameters (Young moduli and Poisson factors) found in [4]. However, in order to match the finite element models to the measured fundamental frequencies, the longitudinal elastic modulus was tuned for each bar. In most of the cases a change of $< 10\%$ of the original value gave a satisfactory result, but for the two lowest and highest notes the Young modulus need to be lowered by as much as 30% compared to the reference value. This highlights the uncertainty of the material parameters. After tuning the fundamental mode,

| | Frequency [Hz] | | | Q-factor | |
|---|---|---|---|---|---|
| Res. | Meas. | Sim. | Lossy | Sim. | Lossy |
| 1 | 305.5 | 328 | 327 | 18.22 | 16.35 |
| 2 | 386.5 | 399 | 397 | 11.08 | 10.45 |
| 3 | 559.0 | 556 | 553 | 9.75 | 8.78 |
| 4 | 641.5 | 640 | 636 | 7.03 | 6.49 |
| 5 | 740.5 | 751 | 748 | 5.11 | 4.79 |
| 6 | 1007.5 | 1024 | 1020 | 3.41 | 3.40 |

**Table 1:** Measured and simulated natural frequencies and quality factors of the cavity resonators

the frequencies of the second and third vertical bending modes did not match perfectly with the measurements, but the average errors were found to be only 2.7% and 6.5%, respectively.

In Figure 3 the 1 : 4 : 10 tuning ratio of the first three vertical modes is clearly visible. The 1 : 4 ratio is achieved quite well in the whole range, whereas the 1 : 10 ratio decreases gradually to 1 : 7 in the upper range H4–A5. This result is explained by the fact that in order to keep the width and thickness of the bars constant along the scale, the length of the undercut must be decreased to keep the 1 : 4 tuning.

## Natural frequencies of the resonators

The resonance properties of the six cavity resonators of the xylophone model were simulated by exciting the acoustical model by an external point source. The results of the simulations are compared to measurements in Table 1. Very good correspondence is seen, in case of the $4^{\text{th}}$ resonator the difference is only 1.5 Hz, while the highest relative difference is 5%.

Due to the relatively large area of the neck of the resonators, the quality factors decrease significantly with increasing the frequency. When the wall losses due to viscosity are also incorporated into the model, the resulting frequencies and Q-factors become slightly lower. As the radiation losses are already greater at higher frequencies, the effect on the Q-factors is greater for the lower resonators.

## Effects of the non-linear interaction

When examining the fully coupled model excited by the hit with the mallet, changing the position or the strength of the excitation can be both expected to have a huge influence on the radiated sound. The time histories of the interaction force are displayed in Figure 4 with changing the initial velocity of the mallet head. As observed, higher velocities result in greater maximum of force. At the same time, the interaction time is decreasing, due to the non-linear force–compression relation (7). Shorter interaction time also means higher cut-off frequency, thus, stronger hits by the mallet can more efficiently excite higher modes of vibration. Thus, both the loudness and the timbre are affected by the strength of the hit.

## Changing the position of the excitation

Figure 5 shows the radiated sound spectra with changing the position of the excitation. The upper diagram shows

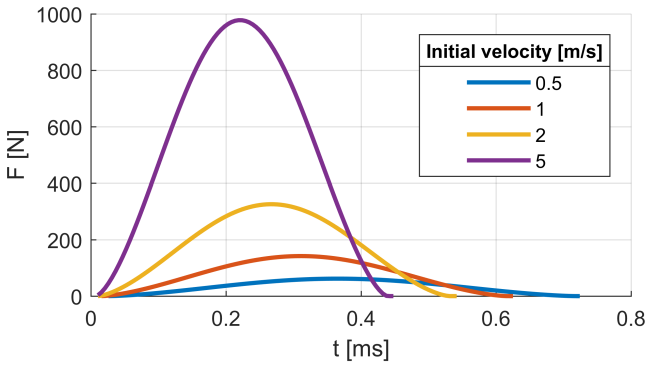


**Figure 4:** Time histories of the interaction force of a hard mallet head and a sound bar with changing the initial velocity

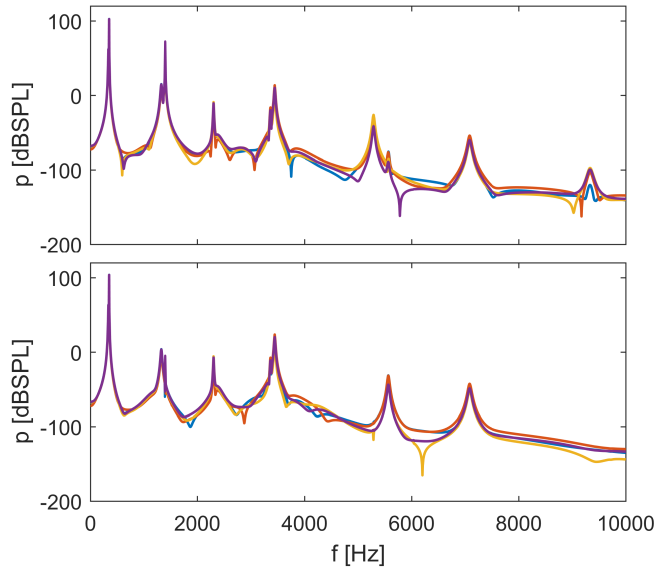


**Figure 5:** Radiated sound spectra when hitting the bar near its end (upper) and at the middle (lower)

the case when the mallet hits the bar near to its end, while in the lower diagram the mallet hits the center of the top surface of the bar. In the second case the second partial has much lower amplitude and a partial around 9.5 kHz is also missing. At the mid-length of the bar the even vertical bending modes have a nodal line and these modes are not excited. Hence, changing the position of the excitation results in a change of the timbre.

The four different colors in each diagram correspond to listener positions at different angles. As seen, the directivity does not have a significant effect in this case.

## Energy relations of the coupled system

The coupled finite element simulation allows for analyzing the energy relations of the subsystems. For the purpose of this analysis, the simulation is divided into two stages: interaction and free vibration. The energy relations in the two stages are shown in Figure 6, side by side. The green curves show the total energy, with the kinetic energy left in the mallet head not shown in the free vibration stage. As observed, the model perfectly preserves the total energy.

It is visible on the left diagram how the energy of the

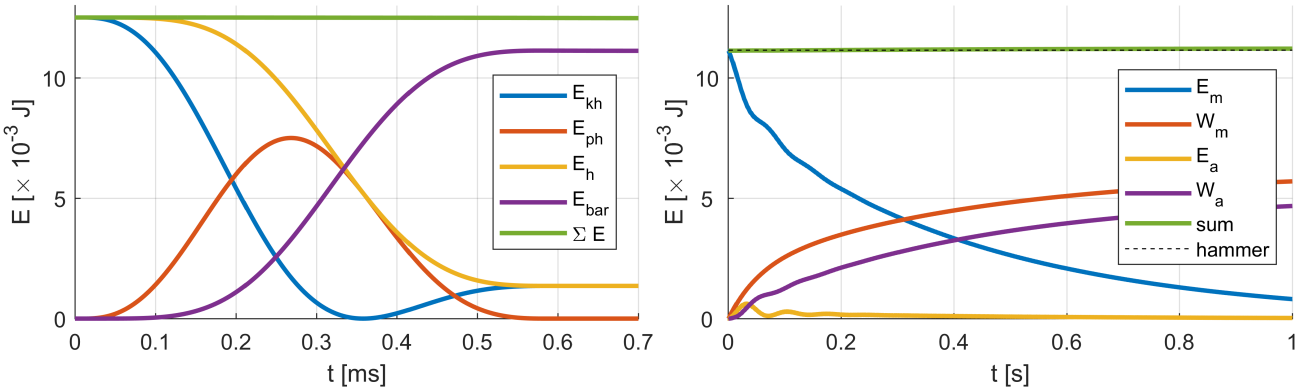


**Figure 6:** Energy relations of the subsystems of the coupled model during interaction (left) and free vibration (right)

mallet head (orange curve) is transferred to the bar (purple curve) during the interaction. The hammer head can store both kinetic (blue curve) and potential (red curve) energy. Interestingly, the minimum of kinetic and maximal of potential energy is not found at the time instance, which can be attributed to the motion of the sound bar.

On the right hand side, the free vibration stage is visible. Initially, only the sound bar has mechanical energy (blue curve), which is transferred to acoustical energy stored in the sound field (yellow curve), radiated acoustical energy (purple curve), and also dissipated by the internal losses of the sound bar (red curve). The dashed line shows the energy entrained by the hit with the hammer. In this case the resonator is untuned and hence only a relatively small portion of energy is radiated into the far field.

## Tuning the resonator

On the original xylophone model one cavity resonator served multiple (2 or 3) sound bars. However, better tuning can be achieved if each sound bar has a dedicated resonator. When the resonator is perfectly tuned to the associated sound bar, such that their fundamental frequencies are almost equal, the energy relations change strikingly compared to that visible in Figure 6. The mechanical energy stored in the sound bar decays much faster, while a high amount of acoustical energy is radiated rapidly and much less mechanical energy is dissipated by the internal losses of the bar. As expected, the sound pressure level becomes remarkably higher in the tuned case, and the decay time decreases drastically, as shown in Figure 7. These results underpin the importance of the proper tuning of the resonator, as it assures efficient radiation and a pleasant decay of the sound.

## SUMMARY

A coupled 3D finite element model was introduced in this paper for examining the design and sound production of a xylophone. The comparison of simulated and measured natural frequencies of sound bars and resonators shows very good agreements. Using the coupled model, various interesting examinations were demonstrated, such as changing the parameters of the excitation, the tuning of the resonator, and the analysis of the energy relations of the system. Finally, the proposed model is also suitable for physics-based sound synthesis purposes.

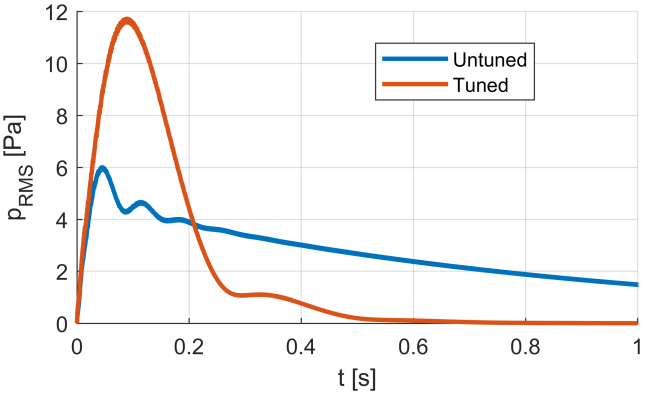


**Figure 7:** Sound pressure levels radiated by a struck xylophone bar coupled to a tuned and an untuned resonator

## Acknowledgments

P. Rucz acknowledges the support of the Bolyai János research grant provided by the Hungarian Academy of Sciences. Supported by the ÚNKP–19–4 new national excellence program of the Ministry for Innovation and Technology.

## References

[1] R. J. Astley, G. J. Macaulay, J-P. Coyette, and L. Cremers. Three-dimensional wave-envelope elements of variable order for acoustic radiation and scattering: Part I. Formulation in the frequency domain. *Journal of the Acoustical Society of America*, 103:49–63, 1998.

[2] A. Chaigne and V. Doutaut. Numerical simulations of xylophones. I. Time-domain modeling of the vibrating bars. *Journal of the Acoustical Society of America*, 101(1):539–557, 1997.

[3] N. M. Newmark. A method of computation for structural dynamics. *ASCE Journal of the Engineering Mechanics Division*, 85:67–94, 1959.

[4] USDA Forest Products Laboratory. Wood handbook: Wood as an engineering material. `https://www.fpl.fs.fed.us/documnts/fplgtr/fpl_gtr190.pdf`, 2010.